Supplementary materials

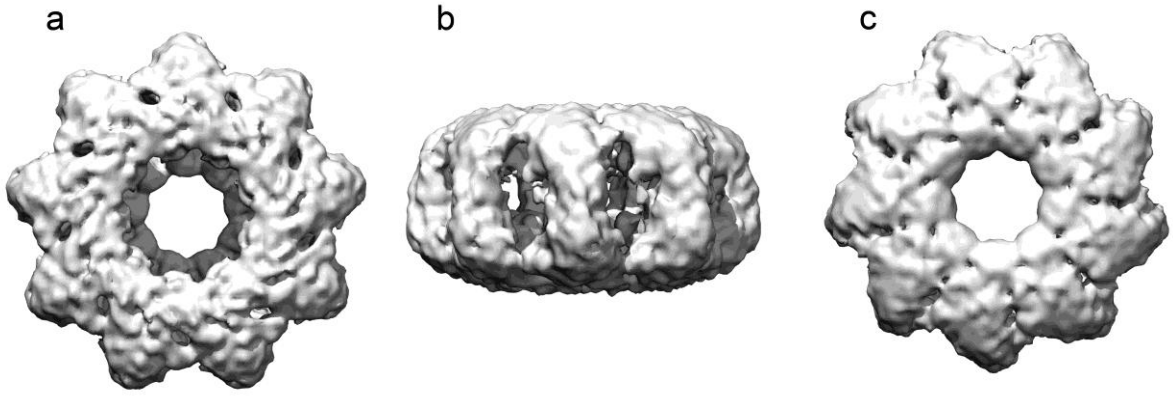

Supplementary figure 1: Initial model used for 3D refinements, which was reconstructed from the reference-free 2D class averages.

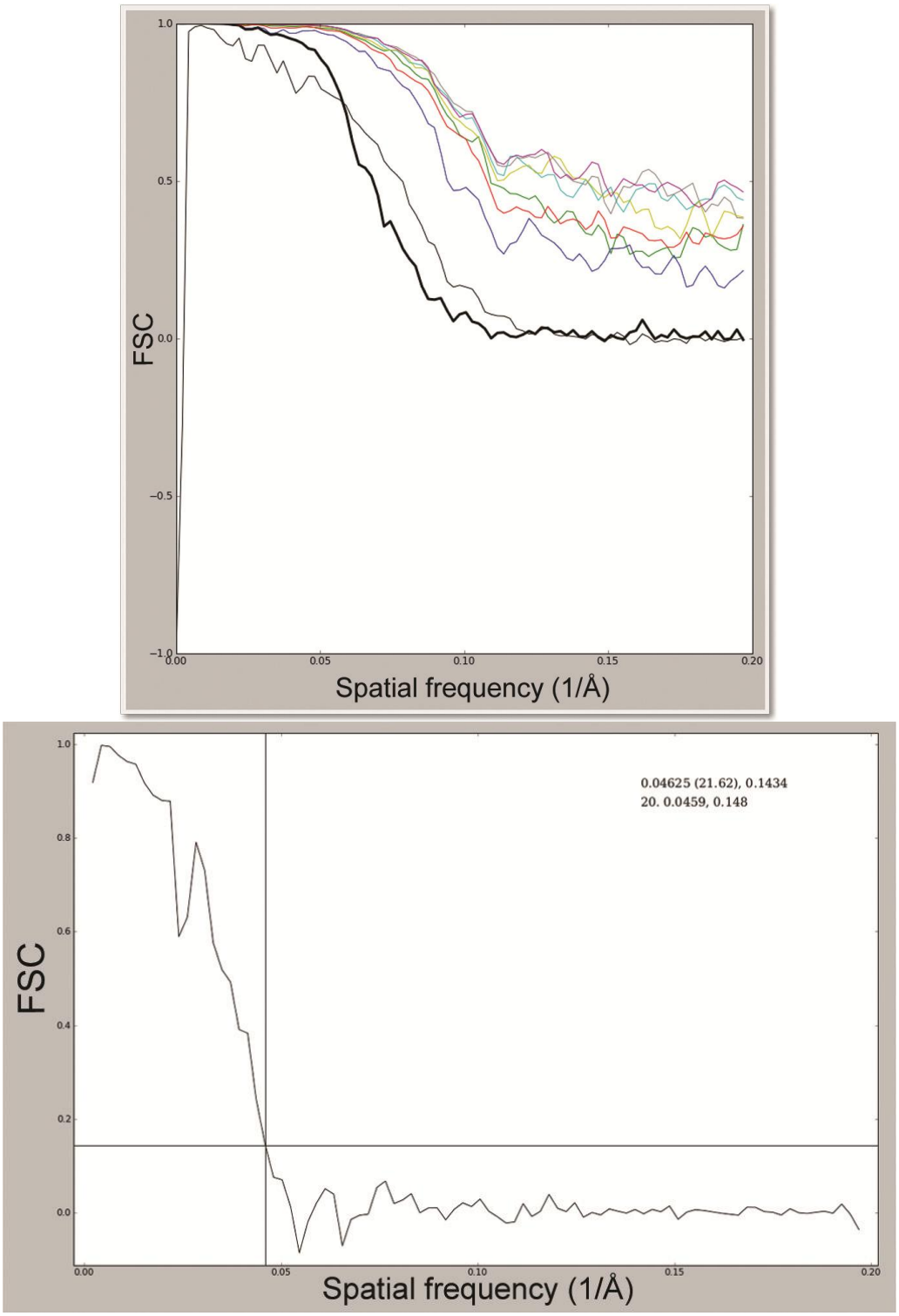

Supplementary figure 2: Top: FSC Curves of iterations and even-odd test. Each thin line represents a 3D refinement iteration, progressively getting better with each successive run, until reaching convergence. The thick black line is of an even-odd test run. Bottom: FSC curve of the golden-standard test used for resolution determination.

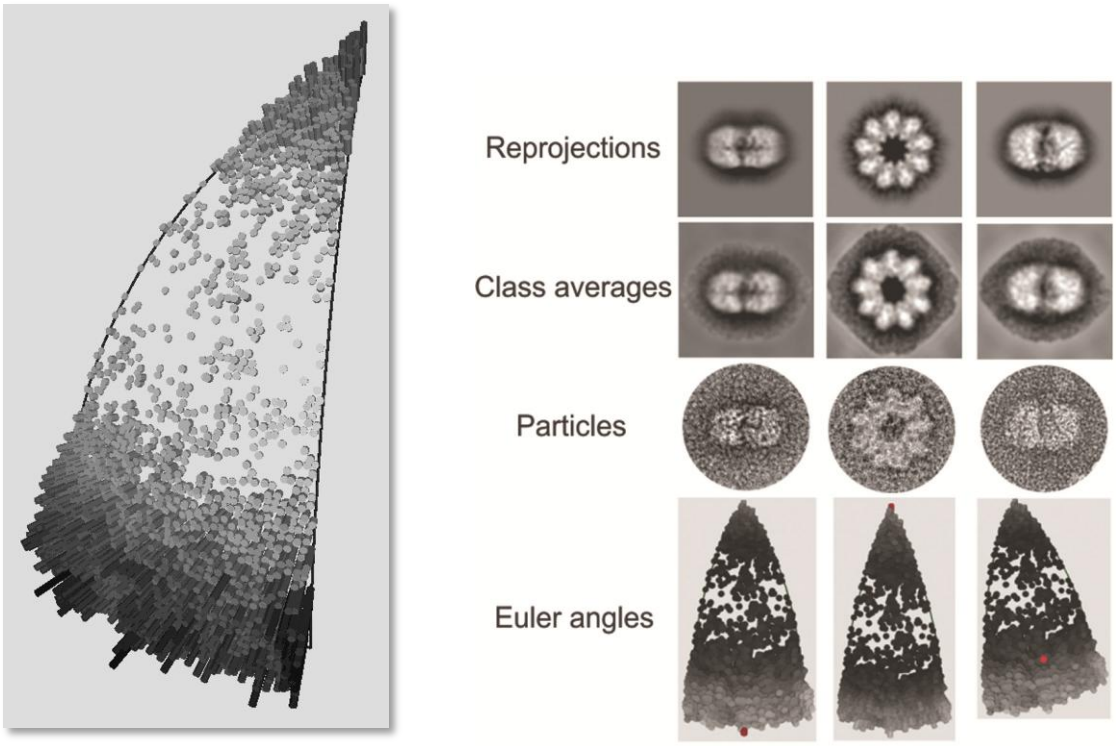

Supplementary figure 3: Left panel: Euler angle distribution of raw particles showing the frequencies of angular assignments of the particles used in the reconstruction. Right panel: comparison of reprojections, class averages and particles at three different Euler angles denoted by the red dot in each frequency distribution. The similarity between reprojections, 2D class averages and raw particles is demonstrated.

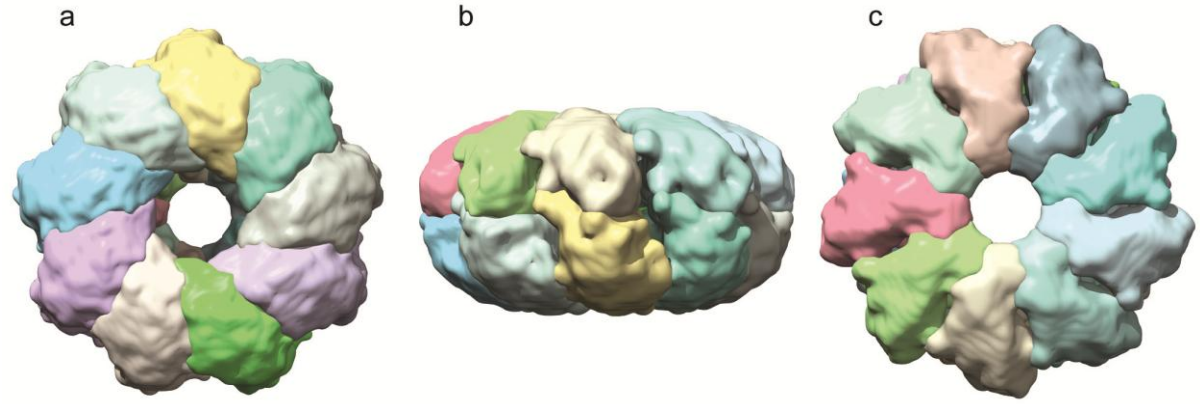

Supplementary figure 4: Segmentation of the map. Sub-volumes used for fitting an ICP8 monomer was determined by density-based volume segmentation in Chimera, each represented by a different color. C9 symmetry is shown in the top and bottom views in panels c and a respectively. Top and bottom layers are visible in side view seen in panel b.

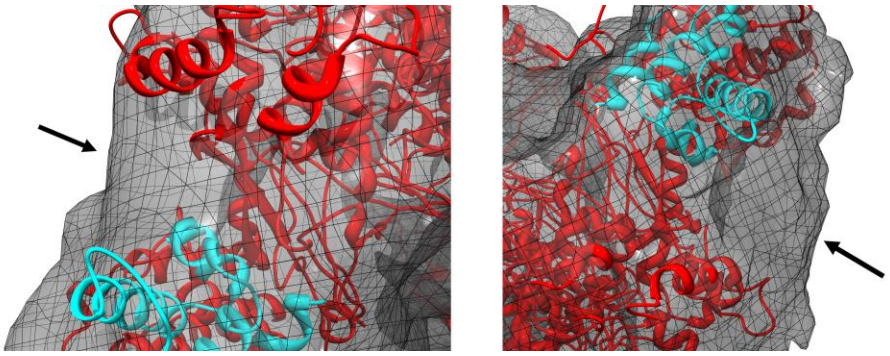

Supplementary figure 5: Arrows point to unoccupied densities around the C-termini after fitting the truncated ICP8 crystal structure. Left and right are from the top and bottom of a symmetrical unit, respectively. These extra densities may belong to the truncated portion, since the full-length ICP8 was used for reconstructing the volume.

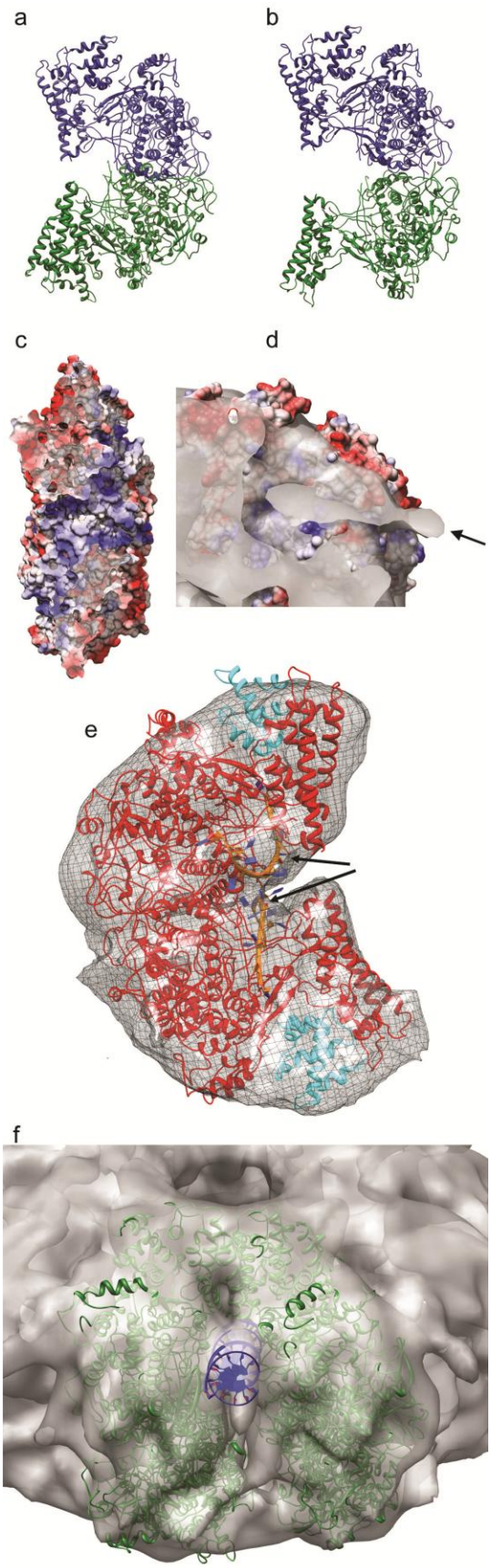

Supplementary figure 6: The comparison between the fitting result shown in a and the crystal packing shown in b. Fitting result in a has an extra C-terminal domain interacting with the bottom monomer compared to the one on the right. Panel c shows the surface charge of one symmetrical unit calculated from the two fitted PDBs showing the surface that faces toward the center of the ring. The surface was clipped to reveal the positively charged surface inside proposed as the ssDNA binding site.In panels c and d, red and blue represent negative and positive charges on the surface charge rendering of the fitted crystal structure, respectively. Panel d shows a side view of a monomer fitted into the top density, which is clipped here to better show the path followed by the extra density, facing the next symmetrical unit. Panel e shows an isolated symmetrical unit with the two fitted PDBs (red and cyan for N and C termini respectively) and the modeled ssDNAs bound to the top and bottom monomers (rendered as orange ribbons). The view point corresponds to the side that faces to the next symmetrical unit. Panel f shows a PatchDock result obtained by docking a straight 20 bp dsDNA (blue) docked to a tetramer of ICP8 (green) fitted into two adjacent symmetrical units. The resulting location of this docked DNA concides with the density protruding from the surface of the ring, which was left unfilled after fitting the crystal structure and shown in detail in Figure 4d and Supplementary figure 6d.

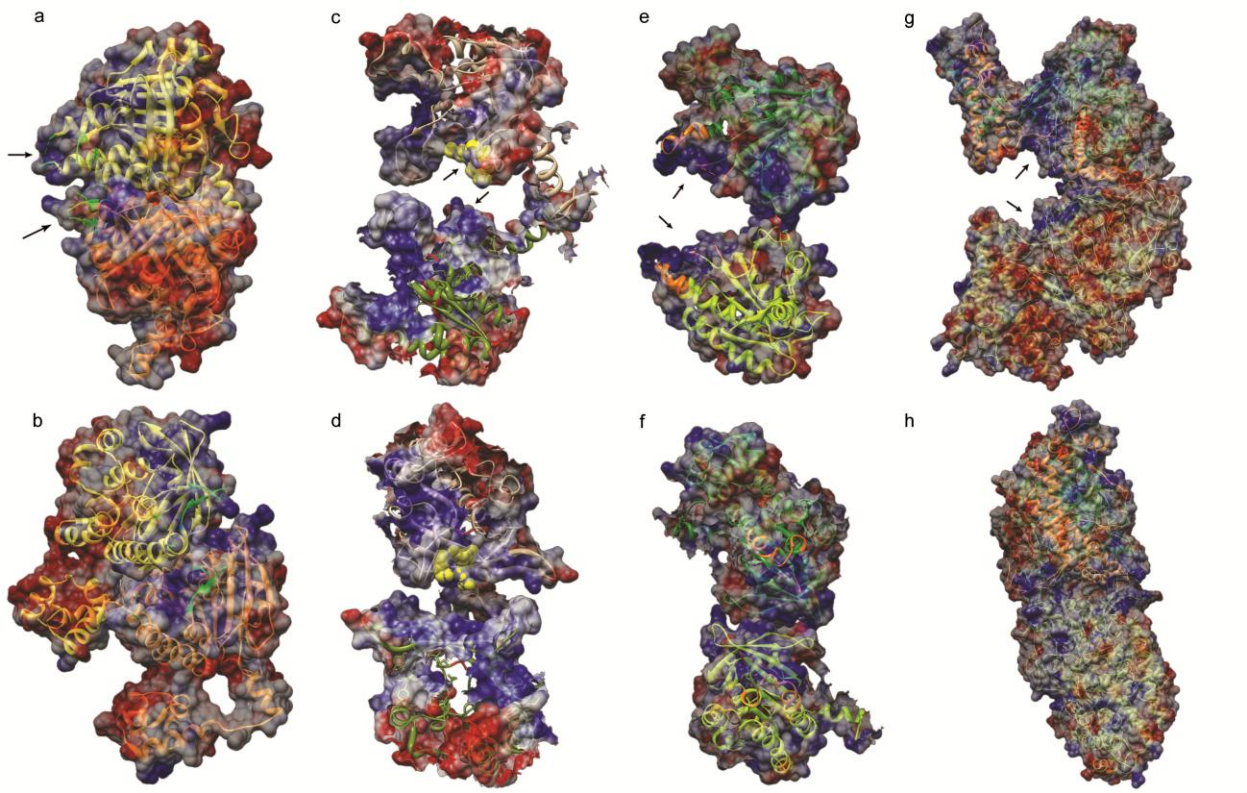

Supplementary figure 7: Comparison of dimer arrangements of recombinases. Top and bottom show the same molecule from the side and front respectively. A, B – RadA; C, D – RecA; E, F – PfRad51; G, H – ICP8. Arrows point to the DNA binding sites of two monomers facing each other.

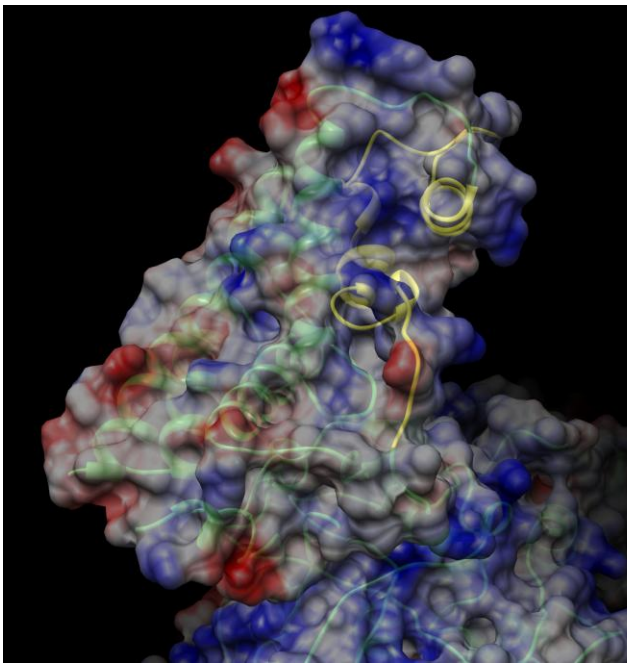

Supplementary figure 8: The predicted secondary DNA binding site of ICP8 shown as a yellow colored ribbon in surface charge representation (positive to negative charges were colored from blue to red).

Supplementary video: Animation (artistic rendering) showing one of the two models proposed for the mechanism of annealing in which ssDNA binds to ICP8 first, forming rings which then dock into each other to catalyze DNA annealing.